OPEN ACCESS

Andreas T. 2026; 1(1) 101-108
DOI: 10.71010/2026.jstrs-e101

Research Article

Journal of Science and Technology Research & Studies

Design of A Resonant Converter Control Loop Using PSIM And Smart CTRL Software

By Topalis Andreas*

Supervisor: Ganatsios Stergios, Department of Electrical and Computer Engineering University of Western Macedonia Faculty

***Corresponding author:** Topalis Andreas, Email: satan131984@hotmail.com

Citation: Andreas T (2026) Design of A Resonant Converter Control Loop Using PSIM And Smart CTRL Software. *J Sci Tech Re Stud*: JSTRS-101. https://doi.org/10.71010/2026.jstrs-e101.

Received Date: May 26, 2026; **Accepted Date:** June 05, 2026; **Published Date:** June 11, 2026

Abstract

An approach on how to design controllers for a bidirectional tuned converter of the CLLLC arrangement is presented in this paper. The ability to achieve zero current switching (ZCS) in all components of this architecture, combined with the ability to operate at very high frequencies, results in improved overall system efficiency. However, the transient behavior of this converter is strongly load dependent, which complicates the design of closed-loop voltage and current regulators. The oscillation noted within the arrangement stems mainly from the Q-factor of resonance being quite large, a feature demonstrably present on the Bode diagram when the loop is open. In this paper, a comprehensive approach to the design of the controller is presented, which takes into account the dynamic response parameters arising from load fluctuations. The robustness of the controlled system will be judged over the entire frequency range in which the switching operation occurs. There will be an extensive report and detailed investigation of both the energy disposal processes in the storage device and the corresponding storage (regeneration) processes. The core novelty presented in this research pivots upon pinpointing the most challenging operational regimes for the converter. This target will be met by employing a systemic approach to modeling and subsequent analysis. Moreover, the choice of the appropriate controller will directly stem from these identified operational characteristics. The verification via the step response demonstrated that, as constructed, the system maintains stability, thus validating the dependability of the control design methodology we put forth. [1]

***Keywords**: DC-DC power converters, bidirectional power flow, tuned converters, control design, battery charger, closed-loop systems.*

1. Introduction

In this study, for CLLLC resonant converters, a technical methodology is laid out focusing on the controller's architecture. This approach is designed to maintain its efficiency over a variety of voltage configurations, both at the input and output. Given that the operational characteristics of these transformation units are subject to alteration based on variations in the connected load, ensuring correct earthing for the control apparatus becomes an absolute necessity. Otherwise, Instability might manifest within the closed-loop system for particular operational settings. To pinpoint the condition posing the most substantial challenge, and concurrently to engineer the regulator guaranteeing stability, an assessment employing frequency response methods shall be leveraged. Specifically, A dual set of control loops, one for voltage and one for current, shall be engineered, concurrently displaying the stability margins guaranteeing operational soundness. The models for the IPT system [2], encompassing both its static condition and the linearized small-signal examination, are derivable and applicable with efficacy to this particular converter configuration. For confirming the prescribed design approach, a physical instantiation of the hardware has seen its creation and assembly. The resulting measurements emphatically establish the efficacy of this methodology. While first noted in reference [3], a more detailed exposition and comprehensive analysis of the subject matter resides herein.

The CLLLC topology resonant converter is depicted in Figure 2. This particular converter formulation allows for two-way power flow. The initial section generates an oscillating signal at a high repetition rate. This signal then traverses the carefully tuned resonant circuit arrangement, its sole purpose being to filter out everything except the primary frequency component, which is then directed toward the secondary part. On the secondary side, this signal undergoes rectification and subsequently feeds the connected load. Furthermore, the transformer serves the crucial role of establishing electrical isolation between the primary and secondary circuits. Its winding ratio is designable and can be modified to permit an enhancement (a step-up) of the overall voltage transformation factor when required. [1]

Therefore, deriving the transfer function for a resonant converter presents challenges. This presentation's core objective is to illustrate that the specified converter permits modeling based on input data gleaned from PSIM AC sweeps, thereby enabling the design of the resonant converter's control loop employing utilities like SmartCtrl.

This case study highlights how powerful and adaptable SmartCtrl is when combined with PSIM, especially for designing the control system in each power converter.

Initially, it is required to extract the frequency response of the resonant converter, which is achieved by using AC analysis in PSIM.

2. AC scan analysis

Performing AC analysis in PSIM

The frequency response of the installation is extracted directly from the tuned converter circuit, through the AC analysis supported by PSIM; no intermediate model is required. The converter circuit is illustrated in Figure 2:

To perform AC analysis, the following are necessary: the AC scanning element, the AC source (for signal input), and the corresponding AC sensor.

Regarding the configuration of the AC leakage, the parameters given in Figure 1 should be followed.

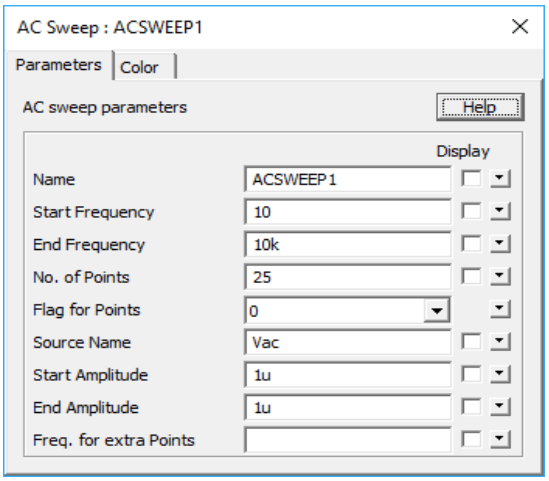

Figure 1: AC analysis configuration.

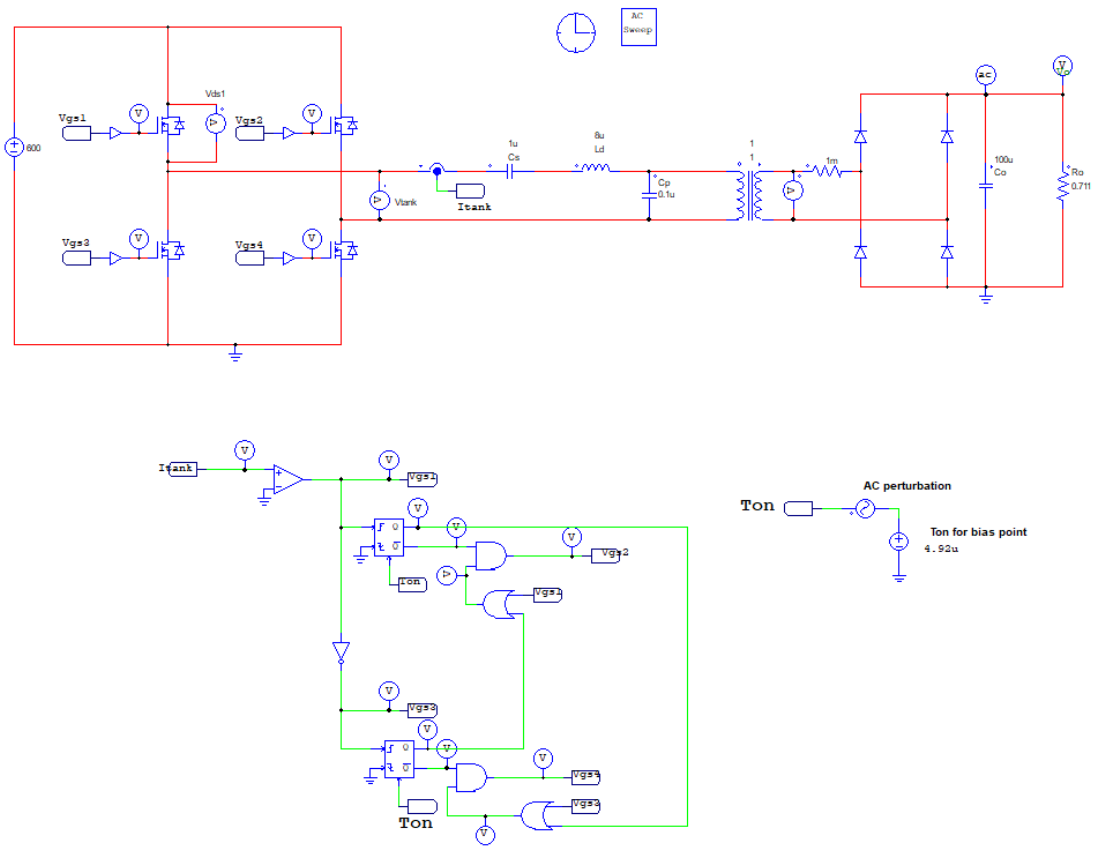

Figure 2: Schematic circuit involving AC sweep.

After conducting the simulation, the response frequency of the output voltage is obtained in relation to the control parameter Ton, as depicted in Figure 3. With the response frequency now available, it is possible to load it into SmartCtrl. [5]

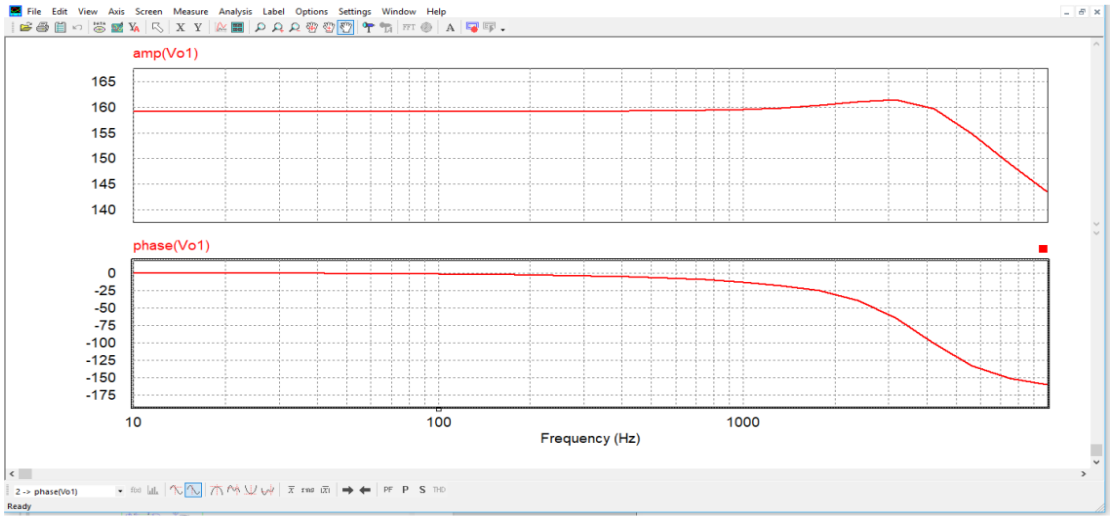

Figure 3: The frequency behavior analysis of the resonant circuit.

3. Control design in SmartCtrl

Enter the frequency response data into SmartCtrl

We click the SmartCtrl button shown in Figure 4 to open SmartCtrl. This action sends the frequency response data from the PSIM AC analysis to SmartCtrl. Upon inputting the desired output voltage and the switching frequency, one proceeds by selecting the "OK" button to advance. (Figure 5).

Figure 4: Access with SmartCtrl shortcut.

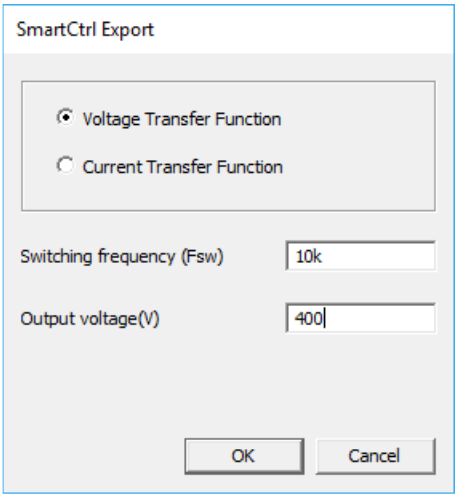

Figure 5: Export to SmartCtrl options window.

The loaded transfer function is automatically plotted as shown in Figure 6.

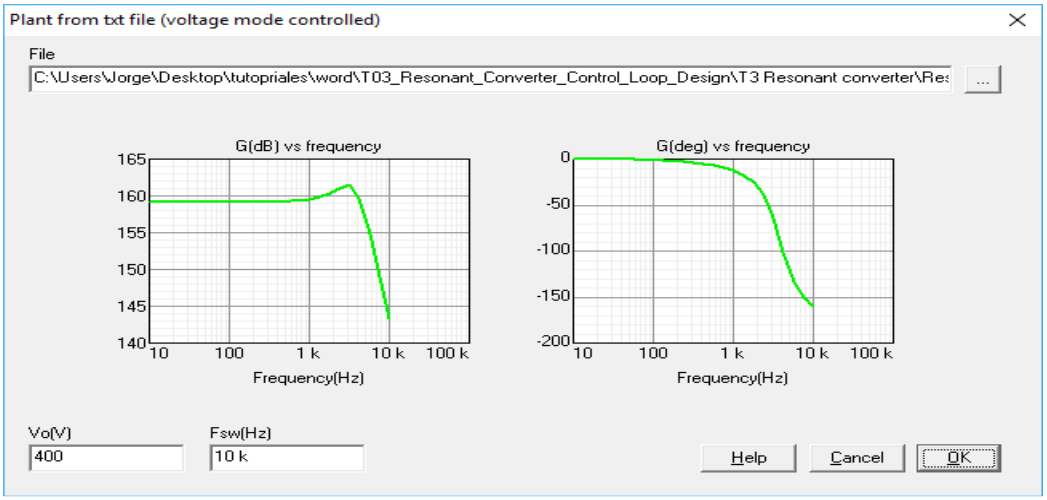

Figure 6: Imported transfer function.

The configuration phase is now entirely wrapped up, the AC sweep having been drawn in from the PSIM tool. The subsequent steps will pivot to defining the parameters for both the sensor and the control mechanism. Look toward Figure 7 for illustration.

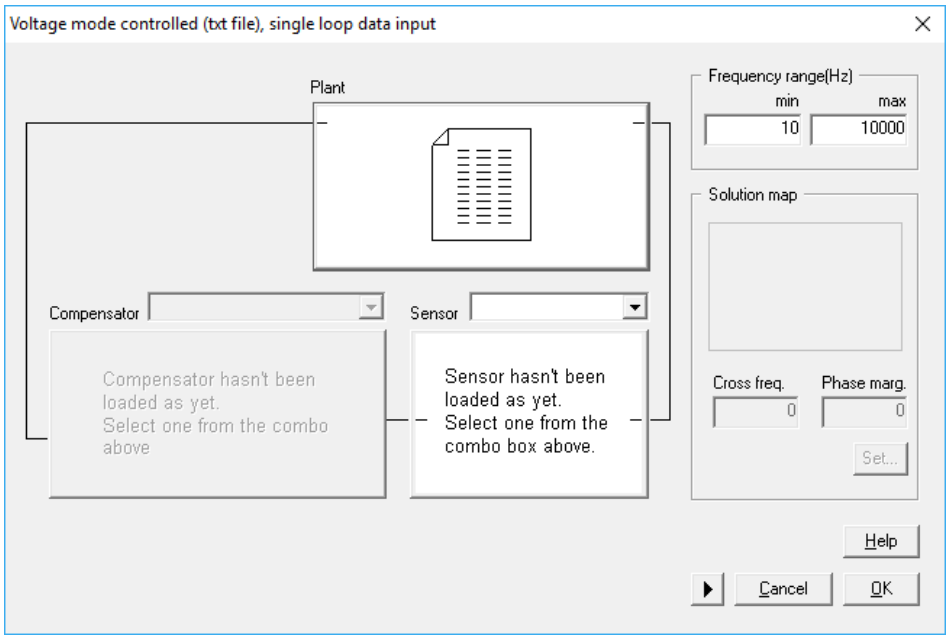

Figure 7: Fully imported facility transfer function.

We click on the sensor tab and select a "voltage divider" sensor topology. We enter a reference voltage of **4.89uV** and click on the "calculate gain" button. We refer to Figure 8.

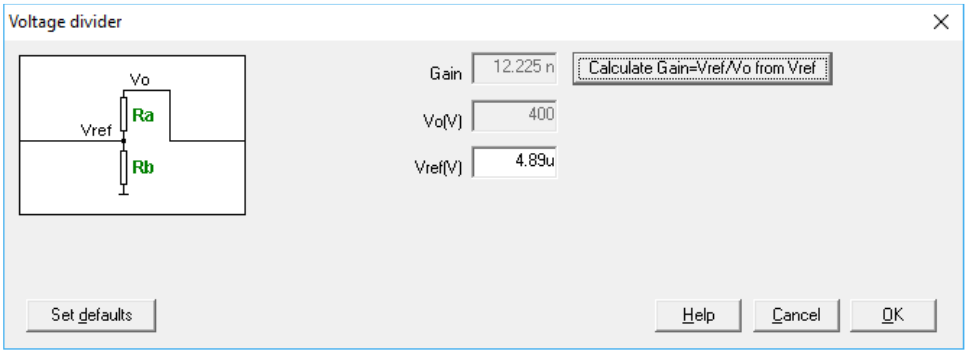

Figure 8: Sensor definition.

To customize the controller, click the "Controller" tab, select a PI type controller and set its parameters exactly as shown in Figure 9.

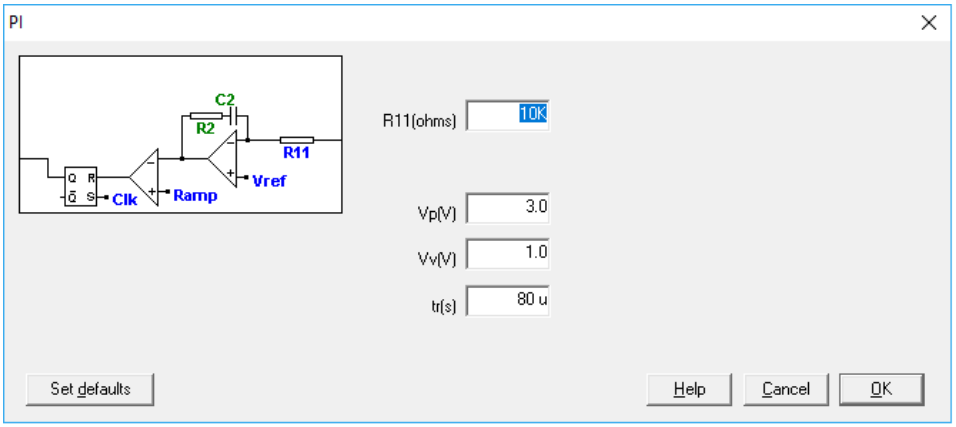

Figure 9: Compensator definition.

Once all the necessary elements of the control loop are defined, the critical selection of the crossover frequency and phase margin becomes possible. The SmartCtrl system offers guidance and a simplified mechanism for selecting these parameters (crossover frequency and phase margin) through the use of the "Solution Map".

The set of points contained in the white space forms a corresponding one for each crossover frequency and phase shift pair, which results in a rigid response. In addition, at each sampled location, there manifests the degradation attributed to both the sensing apparatus and the regulating mechanism, quantified according to the operative cycle rate.

We observe that insufficient suppression of the movement frequency may lead to high-frequency oscillations.

To proceed with the selection, press the "Define" button and SmartCtrl will display the visualization of the solutions. After that, select a point within the white space with the left click and press "OK" to continue. In this article, the crossover frequency of **4.235 kHz** and the phase margin of **72.6** degrees were determined.

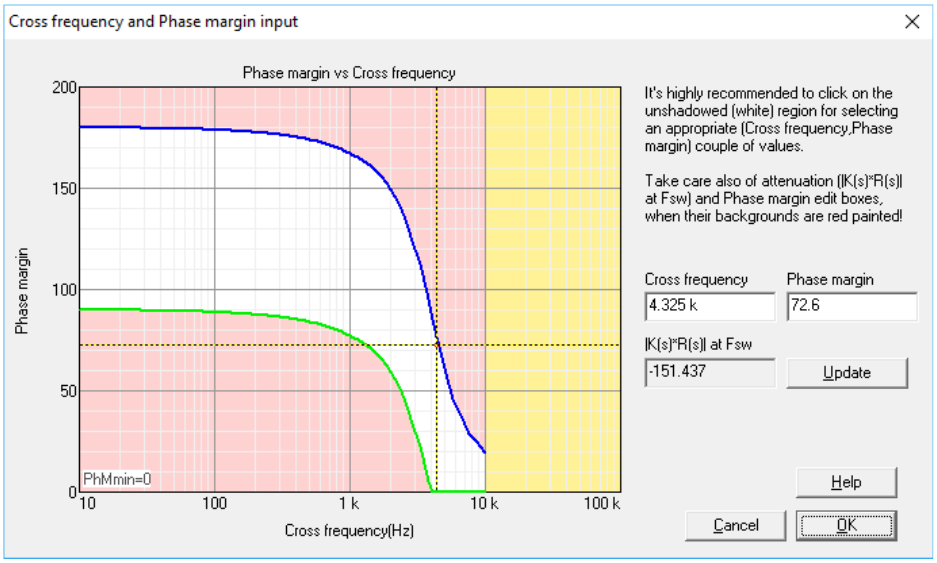

Figure 10: Solution map view.

Once the crossover frequency and phase limit have been selected, the map showing the solutions will become visible on the right side of the data entry box. Should it be necessary to change these two quantities at any time, a simple selection (click) on the already displayed solution map is sufficient.

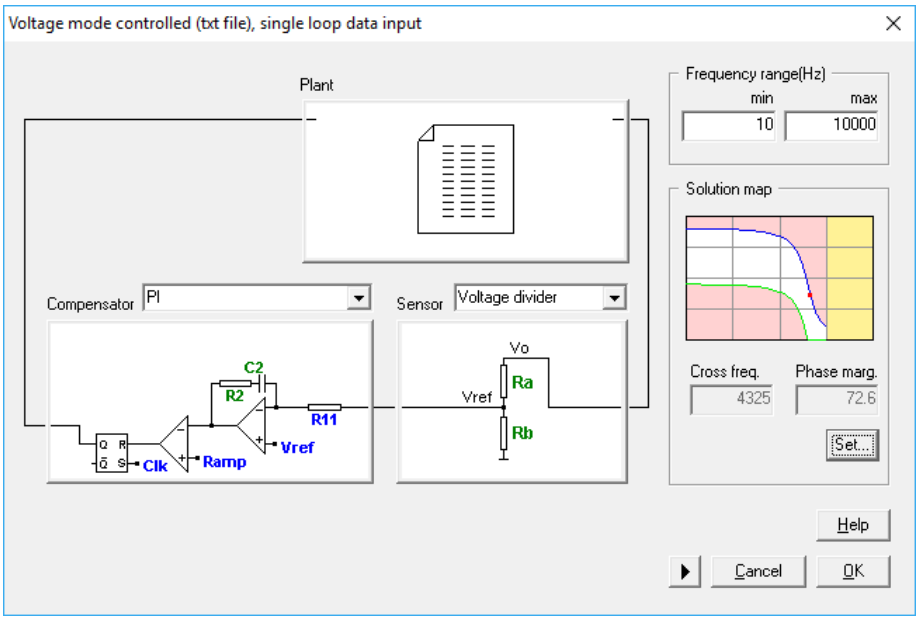

Figure 11: SmartCtrl loop with all elements fully defined.

We proceed to validate the configuration you have chosen and give the green light to the design. The application will take care to immediately present you with the results of the systemic behavior, regarding the frequency response as well as the response to changes. Always remember that the display area of the response diagram remains permanently visible.

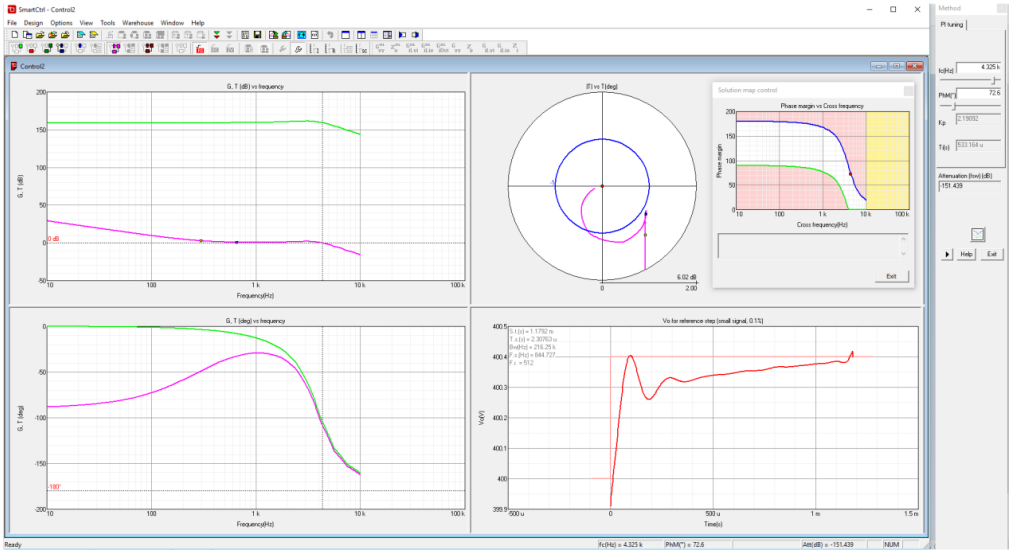

Figure 12: SmartCtrl loop solution.

4. Validation

We validate the control loop design

For the purpose of ascertaining how the closed-loop amalgamation, incorporating the controller formulated via SmartCtrl, behaves, a simulation tracing its operation within the time domain is executed inside the PSIM environment.

Two distinct design configurations are produced by SmartCtrl. The following table presents the control loop bandwidth (BW) and phase margin (PM) for these two implementations, along with the corresponding controller parameters.

Design 1	**Design 2**
Bandwidth = 3.5kHz Phase margin = 55º	Bandwidth = 1kHz Phase margin = 90º
K_p = 1.198 K_{int} = 38.92u	K_p = 471m K_{int} = 35.56u

From Figure 13, these values are derivable via SmartCtrl, as depicted.

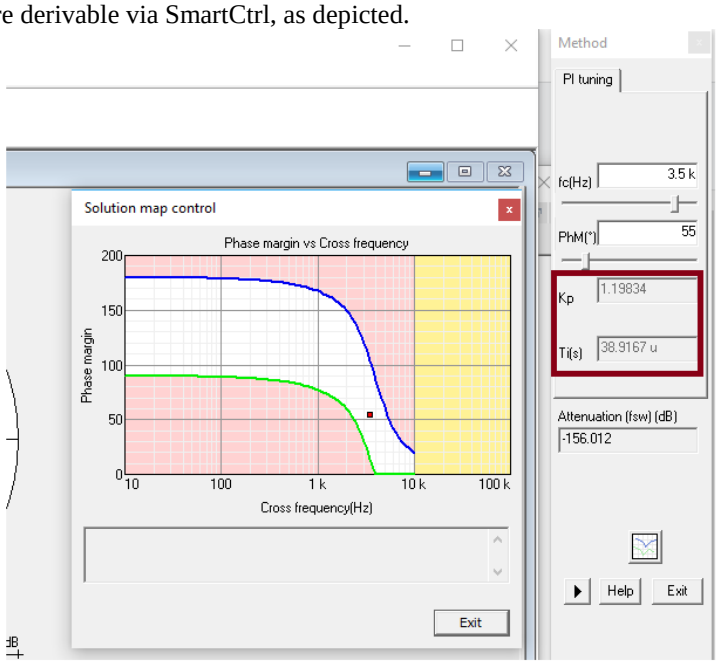

Figure 13: K_p and T_i values extracted from SmartCtrl.

By taking the two controllers listed in the aforementioned table, the corresponding closed-loop behaviors are simulated within the PSIM environment. The PSIM setup is presented in Figure 14. In this setup, at the **5ms** mark, a sudden shift in the incoming electrical potential was applied, this action taken to probe the temporary reaction characteristics of the fabricated control mechanism.

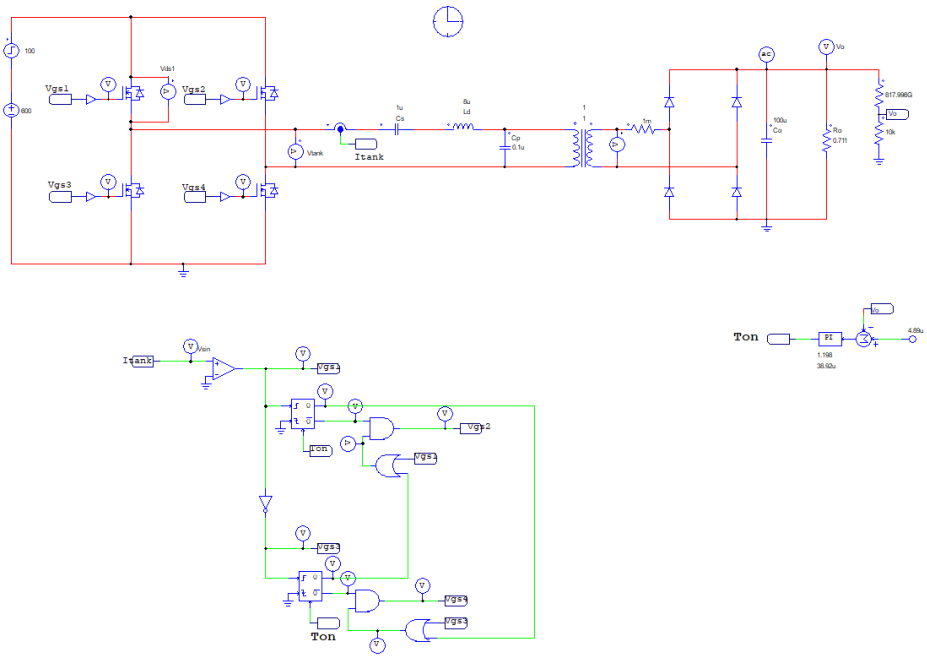

Figure 14: PSIM schematic diagram including input voltage step.

The findings of the simulation process are presented in Figure 15. As defined, the ultimate electromotive force delivered settles at four hundred volts, and the presentation of this measure illustrates its constancy, even when the incoming electrical pressure experiences an abrupt shift (a discontinuity) of **100V**.

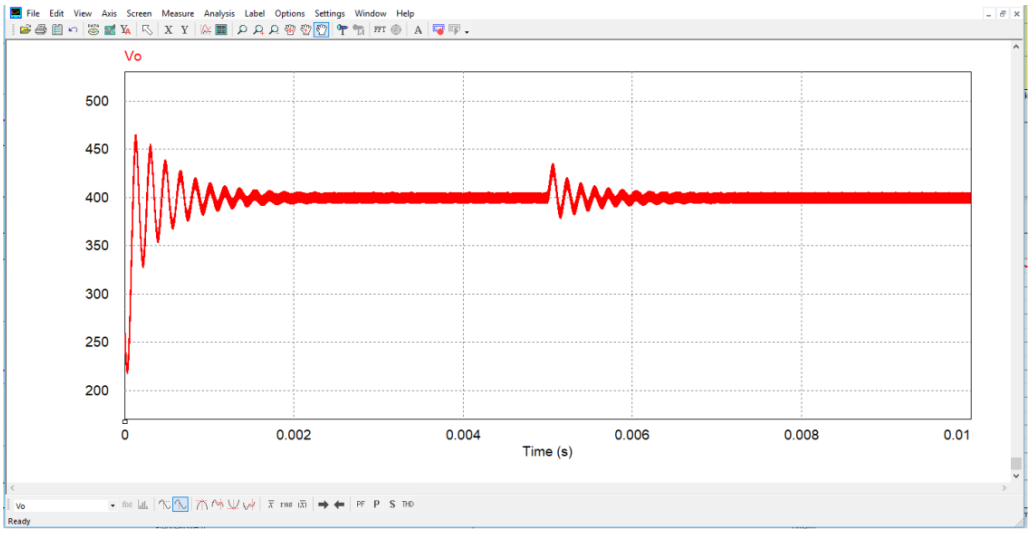

Figure 15: Output voltage.

If the same test is performed again, but using the alternative values of the PI controller (where $\mathbf{K_p}$**=471m** and $\mathbf{K_{int}}$**=35.56u**), it is seen from the waveform recordings that the initial control method (Design 1) exhibits better fidelity in tracking the incoming signal compared to the second approach (Design 2). Although Design 1 has a smaller phase margin, which implies more subdued oscillations, the greater bandwidth achieved, combined with the enhanced gain value at low frequencies, results in achieving a faster system response.

Here we demonstrate how SmartCtrl, when used in conjunction with PSIM – and taking into account the ability to import the frequency response data generated by PSIM – offers a rapid and efficient basis for setting up, improving and fine-tuning control loops for any form of electrical power converter. **[4], [7]**

5. Conclusions

The resonant converter type CLLLC, an eminent design, showcases potent capabilities for highly efficient power transfer, further augmented by the facility for seamless zero-voltage/zero-current transitions across the transformer's initial and final coil sets as for the system's operation, its manner of action shifts dependent upon the settings of the applied stress, thus posing a hurdle in keeping the guiding algorithms steady, making the need for a controller with inherent stability in all possible operating conditions imperative. Herein, this document outlines the process for establishing the parameters reflective of the most adverse situation, and from that foundation, a methodical procedure is formulated for engineering the requisite control mechanism. For the purpose of setting forth outcomes of the design, the acceptable safety zones for each operating case were visually depicted. The control system design for both BCM and RM operation was presented and validated using simulation

and real-world measurement data. The presented figures demonstrated the designed regulation mechanisms suffice for managing the entirety of operational states, whereas the preceding evaluation furnished an in-depth grasp of the resonance characteristics exhibited by the CLLLC converter model. As part of the further development of this study, the implementation of dynamically adaptive controllers could be considered, aiming to maximize bandwidth regardless of conditions. Controllers based on programmed gain are illustrative examples of such adaptive techniques that could be incorporated. [1]

The CLLC circuitry offers a dependable and potent method for transformations of electrical power. The exchange of pulsating energy, occurring dynamically between the inductive and capacitive reservoirs, is what ensures highly effective movement of power from one point to another. Furthermore, the employment of gentle switching methodologies serves to drastically cut down on the energy squandered during the switching instances, therefore boosting the ultimate performance level. Precisely orchestrated timing of the semiconductor elements, achieved through synchronized rectification processes, assures a seamless functional flow and lessens the physical strain endured by the constituent parts. The dual-direction capability of the converter permits energy movement both ways, rendering it ideal for uses involving energy banking and two-way power circulation. For a precise prediction of CLLC converter functionality under diverse operational circumstances, it becomes requisite to construct mathematical models that encapsulate the behavior of the resonant network's constituent parts, the power semiconductor switches, and the implemented control strategies—for instance, the schemes used to hold constant current, constant power, or constant voltage. This very capable converter, whose high marks for operational effectiveness and trustworthiness are clear, owes its success to three primary elements: a reduction in the power shed while transitioning between states, skillfully designed pathways for the flow of energy, and the utilization of gradual transition methods. To cap it all off, the CLLC topology stands as a solid, dependable choice, boasting great efficiency, the capability for two-way power movement, and consistent, error-free functioning. What configures this as the ultimate solution for a broad range of power adjustment necessities is a synthesis of its advanced techniques for energy transport, the reduction to the bare minimum of energy expended during state changes, and the implementation of techniques that soften these transitions. [6].

6. Acknowledgment

My special thanks to my professor Stergios Ganatsios and in general to the entire Department of Electrical and Computer Engineering of the University of Western Macedonia. Regarding the author's contribution with this article I hope for the improvement and development of electric vehicles, renewable energy systems, telecommunications equipment and industrial power electronics.

References

1. Modeling and Controller Design of a Bidirectional Resonant Converter Battery Charger, Zakariya M. Dalala, Zaka Ullah Zahid, Osama S. Saadeh, Jih-Sheng Lai, Received April 11, 2018, accepted April 22, 2018, date of publication April 25, 2018, date of current version May 16, 2018.
2. Z. U. Zahid *et al.*, ``Modeling and control of series_series compensated inductive power transfer system," *IEEE J. Emerg. Sel. Topics Power Electron.*, vol. 3, no. 1, pp. 111_123, Mar. 2015.
3. Z. M. Dalala, Z. U. Zahid, and J. S. J. Lai, ``Modeling and controller design of a bidirectional resonant converter battery charger," in *Proc. Asian Conf. Energy, Power Transp. Electri_c. (ACEPT)*, Oct. 2016, pp. 1_7.
4. C. H. Chang, C. A. Cheng, and H. L. Cheng, ``Modeling and design of the LLC resonant converter used as a solar-array simulator," *IEEE J. Emerg. Sel. Topics Power Electron.*, vol. 2, no. 4, pp. 833_841, Dec. 2014.
5. Infineon Technologies AG: Resonant LLC Converter – Operation and Design.
6. B. Gu, J.-S. Lai, N. Kees, and C. Zheng, ``Hybrid-switching full-bridge DC-DC converter with minimal voltage stress of bridge rectifier, reduced circulating losses, and filter requirement for electric vehicle battery chargers," *IEEE Trans. Power Electron.*, vol. 28, no. 3, pp. 1132_1144, Mar. 2013.
7. A novel digital sensor-less synchronous rectification method for CLLLC resonant converters, Hao Xiea, Chenglin Yangb, Lijun Hanga, Yuanbin Hea, Jiarui Liaoa, Zhen Hea, Pingliang Zenga, Zhaoshen Liu, 2022.